Applied Thermal Engineering 124 (2017) 1–16

Contents lists available at ScienceDirect

Applied Thermal Engineering

journal homepage: www.elsevier.com/locate/apthermeng

Research Paper

Exergo-economic Evaluation of a new drying system Boosted by Ranque-Hilsch vortex tube

Merve Senturk Acar [a,*], Oguz Arslan [b,*]

[a] Tavsanlı Vocational School, Dumlupinar University, 43300 Kutahya, Turkey
[b] Mechanical Engineering Department, Engineering Faculty, Bilecik Seyh Edebali University, 11230 Bilecik, Turkey

HIGHLIGHTS

- The new drying system was designed by integrating Ranque-Hilsch Vortex Tube (RHVT).
- This new system was evaluated by energy, exergy and NPV methods.
- This system was found investable from the economic point of view.

ARTICLE INFO

Article history:
Received 4 March 2017
Revised 23 May 2017
Accepted 4 June 2017
Available online 6 June 2017

Keywords:
Drying system
Economic analysis
Energy analysis
Exergy analysis
Vortex tube

ABSTRACT

In this paper, a new drying system aided by the hot stream of Ranque-Hilsch vortex tube (RHVT) was designed. Then, the designed system was evaluated by means of energy and exergy analysis from the thermodynamics point of view. Finally, this new system was investigated by means of life cycle analysis coupled with the net present value (*NPV*) from the economic point of view. In this aim, several RHVTs with the different geometrical helical generators, control valve angles, RHVT bodies and inlet stream pressures were performed experimentally. The obtained results were evaluated in the designing of RHVT aided drying system (RHVTAD). The highest value of *NPV* of RHVTAD was calculated as 23711.88 € for the $h/w = 0.44$, $d/D = 0.51$, $L/D = 40$, control valve angle of 30°, 3rd control valve opening position. At this case, the operating conditions of this system were T_5 of 328.15 K, T_6 of 308.15 K and P_8 of 601.325 kPa. Under the same circumstances, the energy efficiency of the RHVTAD system was calculated as 0.0348 and 0.0338 while exergy efficiency was calculated as 0.0010 and 0.0023 for the summer and winter modes, respectively.

© 2017 Elsevier Ltd. All rights reserved.

1. Introduction

The vortex tube was discovered by Ranque in 1933 [1] and developed by Hilsch [2]. Ranque-Hilsch vortex tube (RHVT) is a device in which the pressured inlet stream is separated two lower pressure flows including lower and higher temperature profiles in comparison to those of inlet stream [1–5]. The pressured gas stream enters to the RHVT tangentially, then a swirling flow occurs in RHVT body by passing through the helical vortex generator. The hot and cold streams of RHVT were separated from each other by the control valve [1,5–6].

In literature, the energy separation of inlet stream in RHVT was investigated by using numerical techniques and experimental methods [7–15]. Andalibi et al. investigated the effect of orifice diameter and diameter on the performance of the vortex tube for $L = 106$ mm, 3 different D (10, 16, 20 mm) and 4 different d/D values (0.15–0.45–0.55–0.71) by using the Computational Fluid Dynamics (CFD) technique. As a result, they noted that RHVT's best performance was achieved for $d/D = 0.45$ [7]. Chang et al. conducted an experimental study of the vortex tube cooler with the conical hot tube. RHVT energy separation performance can be improved by using a conical hot tube. RHVT energy separation performance can be improved by using a conical hot tube. They stated that the RHVT energy separation performance can be improved by using a conical hot tube. As a result of the work done, they emphasized that it is an optimum angle for obtaining the highest cooling performance and that the optimum angle can be taken as 4° under their own experimental conditions [8]. Dutta et al. examined the phenomenon of energy and species separation in a vortex tube operated with compressed air at normal atmospheric temperature and cryogenic temperature using with a three-dimensional CFD model [9]. There are several studies on the performance of hot

* Corresponding authors.
E-mail addresses: merve.senturkacar@dpu.edu.tr (M. Senturk Acar), oguz.arslan@dpu.edu.tr (O. Arslan).

http://dx.doi.org/10.1016/j.applthermaleng.2017.06.010
1359-4311/© 2017 Elsevier Ltd. All rights reserved.

Nomenclature

C	cost (€)
c	specific heat (kJ/kg K)
$\dot{E}x$	exergy (kW)
h	specific enthalpy (kJ/kg)
i	interest rate (%)
j	discount rate (%)
$\dot{m}$	mass flow (kg/s)
MR	dimensionless moisture ratio
M_e	equilibrium moisture content at any time (kg water/kg dry matter)
M_o	initial moisture content at any time (kg water/kg dry matter)
M_t	the moisture content at any time (kg water/kg dry matter)
n	the numbers of measurement
NPV	Net Present Value (€)
P	pressure (kPa)
ol	operating life (year)
R	air gas constant (kJ/kg K)
$\dot{Q}$	heat energy (kJ/s)
r	discount rate (%)
t_{33}	working time of the system for winter (h)
t_{16}	working time of the system for summer (h)
ω	humidity ratio
T	temperature (K)
U	uncertainty
$\dot{W}$	electrical power (kJ/s)
$\bar{X}$	the average of the measurement
X_m	the measurement
ε	exergy efficiency (%)
ψ	specific exergy (kJ/kg)

Subscripts

a	air
ash	ash
b	benefit
car	carbohydrate
d	destruction
e	electrical
eh	electrical heater
exp	experimental
fat	fat
fib	fiber
fp	fresh product
ic	investment costs
mc	maintenance costs
mec	mechanical
oc	operating costs
pro	protein
$RHVT$	Ranque-Hilsch vortex tube
$RHVTAD$	Ranque-Hilsch vortex tube aided drying
sc	salvage costs
ss	saturated steam
sys	system
T	total
t	time (year)
tom	tomato
v	vapor
w	water
0	dead state
16	winter period
33	summer period

and cold streams of RHVT in which energy and exergy analysis were used [16–22]. Kırmacı investigated the effect of inlet nozzle number and inlet pressure on the cooling and heating performance of counter-flow RHVT by using air and oxygen as a working fluid. As a result of the study, it has been revealed that the cold outlet temperature is decreased by increasing the inlet pressure of vortex tube and the temperature difference between cold and hot flow is reduced by increasing the number of inlet nozzles for both fluids [18]. Cebeci et al. investigated the effects of the orifice nozzle number and the inlet pressure on heating and cooling performance of a counter flow Ranque–Hilsch type vortex tube. They emphasized that the temperature gradient between the cold and hot flow increase with the decrease of the orifice nozzle number increases and the increase of the inlet stream pressure [22]. Also, the optimum operating parameters of RHVT were determined with experimental and numerical methods [23–32]. Dincer et al. examined the effects of control valve angle on counter flow RHVT by using artificial neural networks and experimental data. The best performance was achieved in the case of a control valve with 60° angle [23]. Aydın and Baki conducted an experimental study on the geometrical parameters and performance of counterflow RHVT. As a result of the studies, the optimum RHVT geometrical values at 500 kPa of inlet pressure were determined as 50° of control valve angle, a tube length of 350 mm, tube diameter of 18 mm and inlet nozzle diameter of 6 mm [25]. Markal et al. conducted an experimental study to investigate the effect of the conical valve angle on energy seperation in counter-flow RHVT. They stated that higher efficiency was achieved with small cone valve angles and conical valve angle had less effect on RHVT performance than L/D value [26]. The direct usage of RHVT in the vapor compression cooling system was investigated in many studies for different working fluids and operating conditions [33–36]. In the literature, it is so hard to find a study on the direct usage of a hot stream of RHVT in the drying system. Drying is one of the oldest methods used to store the foods since it prevents the formation of the microorganisms which causes deterioration and decaying of the food. Because of the insufficiency of the long time storage conditions of foods and the requirements of peoples for the energy makes the scientists research the alternative ways. The energy consumed reached up to 29% for the drying process in the food sector [37].

In this study, the new system design was made in which hot stream of RHVT used in the drying system. The effect of hot stream of RHVT on the drying system was investigated with using thermodynamic and economic analysis. The life cycle cost (LCC) method coupled with *NPV* was used to determine the economics of the RHVT aided drying system. The performance of Ranque-Hilsch vortex tube aided drying system (RHVTAD) was investigated for the different operating and geometrical parameters of RHVT. Beside this, the different operating parameters such as the inlet and outlet temperatures of the dryer were also investigated in the view of thermodynamic points, using the energy and exergy analysis methods.

2. Material and methods

In this study, RHVT mainly consists of three components named as the helical vortex generator (A), control valve (B) and RHVT body

(C) (see Fig. 1). The used geometrical parameters of RHVT were chosen as height (h), width (w) of the channel, inner diameter (d) of the helical vortex generators and length (L), diameter (D) of RHVT bodies.

In the experiments, 8 different generators were used. All the helical vortex generators have a single nozzle and 3 different control valve angles were used ($\alpha = 30°$, 45°, 60°). The properties of RHVT used in experiments were summurized in Table 1 [31].

2.1. The experimental set-up of RHVT

The image and schematic diagram of experimental set-up of RHVT were given in Fig. 2 [31]. The air was compressed by a pressure-adjustable air-cooled compressor (a) and then was stored in a pressure tank (b) with a capacity of 0.3 m^3. The volumetric rate of the flow was adjusted by means of a spherical valve (c). The compressed and adjusted air enters to the helical vortex generator (A) and exits as a swirling flow from RHVT body (C). Then, this swirling shape of flow is separated into hot and cold streams in RHVT body by means of the control valve (B).

The pressure and volumetric rate of the cold and inlet streams of RHVT were measured by a relative pressure transmitter (d) and an air flowmeter (f). The volumetric rate of the hot side was calculated using the conservation law of mass. The temperature of the cold stream and compressed inlet air were measured by a PT100 type of thermocouple (d). The temperature of the hot stream was measured by a relative humidity and temperature transmitter (k). All the measured data was then stored in a data logger. The energy consumption of compressor was also measured and stored by a network analyzer integrated to the data logger. The technical properties of the measurement devices were given in Table 2 [31].

The experiments of RHVT were conducted for different inlet stream pressures ranging between 201.325 kPa and 601.325 kPa. The different mass fractions of the hot stream were also included changing the control valve position. In this aim, 4 different positions of control valve opening were taken into consideration. The measurements were evaluated with the uncertainty analysis. The average of the measured values is given by ($\bar{X}$);

$$\bar{X} = \frac{\sum X_m}{n} \tag{1}$$

where n; the numbers of the measurement and X_m; the measured value. Standard deviation (SD) is given as following;

$$SD = \sqrt{\frac{\sum_{m=1}^{n} (X_m - \bar{X})^2}{(n-1)}} \tag{2}$$

Then, uncertainty (U) is given by Eq. (3) as following [38];

$$U = \frac{SD}{\sqrt{n}} \tag{3}$$

The cold and hot streams pressures were accepted as 101.325 kPa since these stream outlet to the ambient. Therefore, the uncertainties of the pressure meters after cold and hot streams were not calculated. The uncertainties of the measurements were given in Table 3. According to the findings of the uncertainty analysis, it was determined that the obtained results of the measurements were acceptable for the use in the design of the RHVTAD.

2.2. Designing of RHVTAD system

The experimental results of the RHVT, electrical heater and page drying model for tomato were used to determine the design parameters of RHVTAD system. The RHVTAD has four main devices; compressor, RHVT, electrical heater, and dryer. The flow diagram of RHVTAD system was shown in Fig. 3.

As seen in Fig. 3, the air enters to the compressor at point 1 and the compressed air inlets to the RHVT (point 2) tangentially. The inlet stream of RHVT splits two flow in RHVT body. The cold stream of RHVT exits from RHVT at point 3 and the hot stream enters to the electrical heater (point 4). The hot stream of RHVT heated to the inlet air temperature of the dryer in the electrical heater. The heated air enters to the dryer (point 5) and takes the moisture of the fresh product which enters to the dryer at point 7. The mixture of air and moisture exits to the dyer at point 6 and the dried product exits to the dryer at point 8. Determination of the drying period and dimensionless moisture ratio (MR) of the tomatoes are mainly based on Page model given by Ref [39]. The moisture ratio (MR) of the samples is determined by the following equation [39];

$$MR = \frac{(M_t - M_e)}{(M_0 - M_e)} \tag{4}$$

where M_t: the moisture content at any time (kg water/kg dry matter), M_0: initial moisture content (kg water/kg dry matter), M_e: equilibrium moisture content (kg water/kg dry matter). The final MR value was accepted as 11% for the dried tomato. So that, the temperature of inlet stream of dryer and drying period were determined by using Page drying model for tomato. The variation of the drying period of tomato versus the temperature of the inlet stream of dryer was given in Fig. 4 [39]. In the designs, the temperature differences of inlet and outlet stream of dryer was adopted as 2 K, 5 K, 10 K, 15 K and 20 K. The inlet stream temperature of the dryer was taken as 328.15 K, 333.15 K, 338.15 K and 348.15 K while the drying period of the tomato took 127,800, 100,800, 95,400 and 86,400 s, respectively [39]. The ambient temperature was considered as 306.15 K for summer period (5 months) and 289.15 K for winter period (7 months).

The summary of designing parameters including the temperatures of the inlet and outlet streams of the dryer, the temperature of the fresh and dried product and drying periods were given in Table 4.

The temperature of the hot stream of RHVT was heated to the temperature of the inlet stream of the dryer using the electrical heater. The efficiency of the electrical heater was determined with the experiments. The electrical wiring diagram of the electrical heater was shown in Fig. 5 [31].

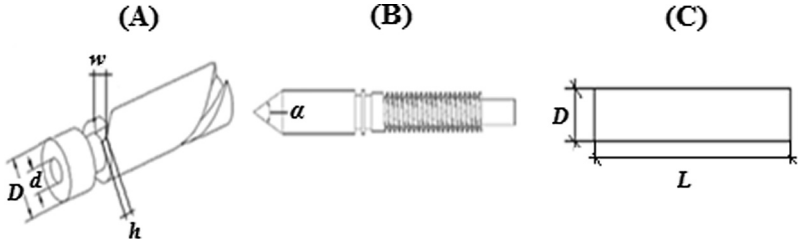

Fig. 1. The illustration of helical vortex generator (A), control valve (B) and RHVT body (C) [31].

Table 1
Technical properties of RHVT [31].

Property	h (mm)	w (mm)	h/w	d (mm)	D (mm)	d/D	L (mm)	D (mm)	L/D	α (°)
	Vortex generator									
A	2.0	4.5	0.44	3.3	12	0.27	–	–	–	–
B				5.1		0.42	–	–	–	–
C				6.1		0.51	–	–	–	–
D				7.1		0.59	–	–	–	–
M	1.5	6.0	0.25	3.3		0.27	–	–	–	–
N				5.1		0.42	–	–	–	–
O				5.7		0.47	–	–	–	–
J				7.1		0.59	–	–	–	–
	RHVT body									
1	–	–		–	–	–	480	12	40	–
2	–	–		–	–	–	350		29.17	–
3	–	–		–	–	–	210		17.5	–
	Control valve									
1	–	–		–	–	–	–	–	–	30
2	–	–		–	–	–	–	–	–	45
3	–	–		–	–	–	–	–	–	60

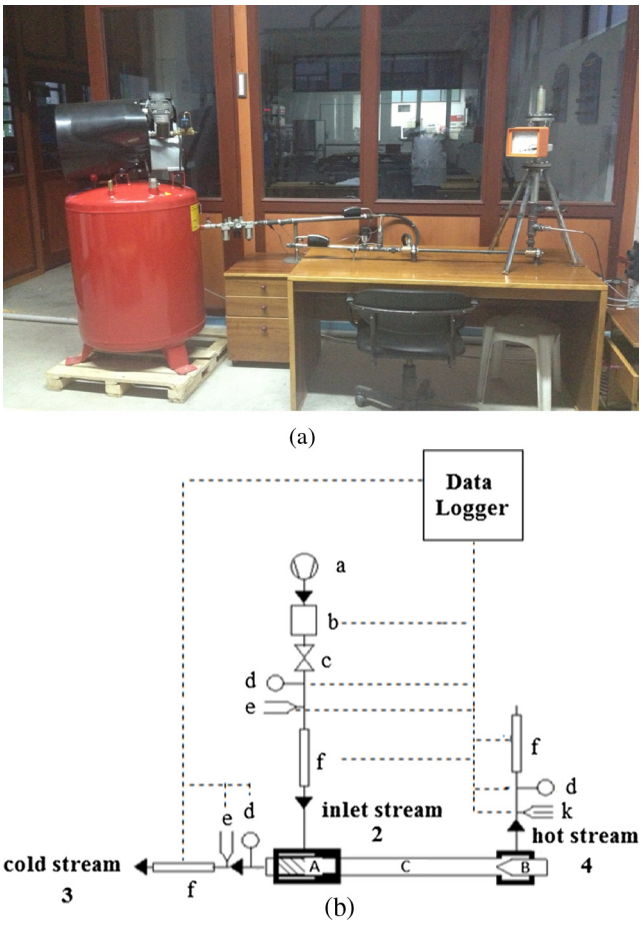

Fig. 2. The image (a) and schematic (b) of the experimental set-up of RHVT [31].

As seen in Fig 5, 13 (500 W) heater resistances were used in the experiments. Here, 4 heater resistances connected in series (three line) and one heater resistance connected to each other line in parallel. The schematic diagram and image of the experimental set-up of the electrical heater are given in Fig. 6 [31].

The air compressed in the compressor (a) and collected in the air pressure tank (b). The flow of the air was setting by a spherical valve (c). The pressure, temperature, and flow of the air was measured with a relative pressure transmitter (d), thermocouple (e) and a flowmeter (f), respectively. After the measurements, the compressed air enters to the electrical heater (g). The temperature and relative humidity of the heated air (h) were measured with relative humidity and temperature transmitter at point k. The consumed power of electrical heater was measured. The electrical heater efficiency was calculated with Eq. (1).

Table 2
Technical properties of the measurement devices [31].

Device	Type	Property	Sensibility
Thermocouple	Testo, PT 100	223.15–573.15 K	±0.05 K
Relative pressure transmitter	WİKA S-10	0–1000 kPa	±0.5% kPa
Flow meter (cold stream)	Testo 6441	0.25–75 $m^3\ h^{-1}$	±3% $m^3\ h^{-1}$
Flow meter (inlet stream)	Testo 6442	0.75–225 $m^3\ h^{-1}$	±0.3% $m^3\ h^{-1}$
Relative humidity and temperature transmitter	Testo 6881	233.15–453.15 K 0–100% RH	±0.2 K ±1% RH
Data logger	Elimko PR-100	12 channel, 85–265 VAC	–

Table 3
The uncertainties of the measurements [31].

Measurement devices	Uncertainty (U)
Thermocouple (T_3)	±0.264 K
Thermocouple (T_2)	±0.445 K
Relative pressure transmitter (P_2)	±5.68 kPa
Flowmeter (cold exit)	±0.218 $m^3\ h^{-1}$
Flowmeter (inlet stream)	±0.303 $m^3\ h^{-1}$
Relative humidity and temperature transmitter (T_4, ϕ_4)	±0.490 K, ±0.154 RH

$$\eta_{eh,exp} = \frac{\dot{m}_a \cdot c_{p,a} \cdot (T_{he,out} - T_{he,in})}{\dot{W}_{exp}} \quad (5)$$

where $\dot{m}_{ei}$: air mass flow rate during the test (kg/s), $c_{p,a}$: specific heat of air (kJ/kg·K), $\dot{W}_{exp}$: consumed electric energy per unit of time (kW), $T_{he,in}$: the temperature of the inlet air in electrical heater (K) ve $T_{he,out}$: the temperature of the outlet air in electrical heater (K). The experimental results of the electrical heater are presented in Fig. 7.

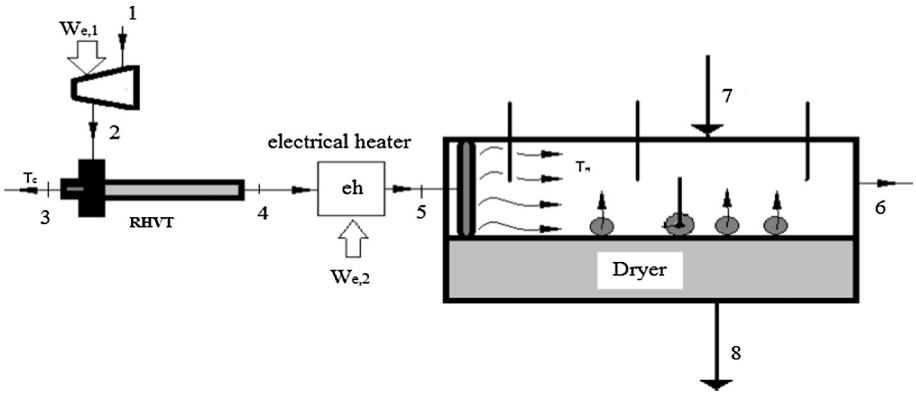

Fig. 3. The schematic flow diagram of RHVTAD system.

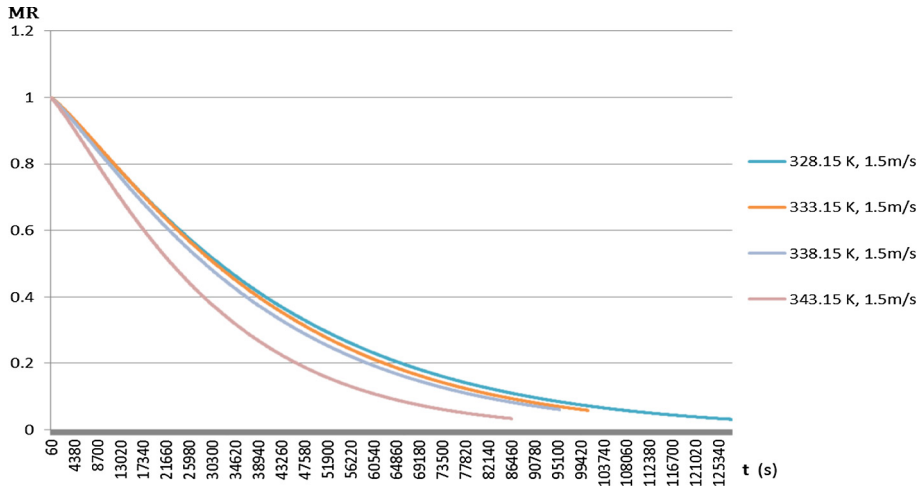

Fig. 4. The variation of the drying period of tomato versus the temperature of the inlet stream of dryer [39].

Table 4
The operating parameters of the dryer.

Drying period (s)	T_5 (K)	T_6 (K)	T_7 (K)	T_8 (K)
127,800	328.15	326.15	293.15	326.15
		323.15		323.15
		318.15		318.15
		313.15		313.15
		308.15		308.15
100,800	333.15	331.15		331.15
		328.15		328.15
		323.15		323.15
		318.15		318.15
		313.15		313.15
95,400	338.15	336.15		336.15
		333.15		333.15
		328.15		328.15
		323.15		323.15
		318.15		318.15
86,400	343.15	341.15		341.15
		338.15		338.15
		333.15		333.15
		328.15		328.15
		323.15		323.15

As seen in Fig. 7, the mean value of the electrical heater efficiency was determined to 0.27 [31]. The inlet air temperature was included in the calculations as equal to the ambient temperature while the power consumption of electrical heater calculated for thermodynamic analysis of the electrical drying system.

3. Energy and exergy analysis of RHVTAD system

In this study, the following assumptions were handled in the energy and exergy analysis;

(1) Steady state conditions were taken into account for all the components,
(2) Pressure losses in the pipelines were neglected,
(3) Potential and kinetic energy effects were neglected,
(4) The electrical heater has an efficiency (η_{eh}) of 27%,
(5) The compressor has an electrical (η_e) and mechanical (η_{mec}) efficiency of 90%,
(6) The reference state is 101.325 kPa and 293.15 K.

Under these assumptions, the governing energy equations for RHVTAD (see Fig. 3) were obtained as follows.

Compressor;

$$\dot{W}_1 = R \cdot T \cdot \ln\frac{P_1}{P_2} \cdot \dot{m}_2 \tag{6}$$

and electrical power of compressor;

$$\dot{W}_{e,1} = \frac{\dot{W}_2}{\eta_{mec} \cdot \eta_e} \tag{7}$$

RHVT;

$$\dot{Q}_{RHVT} = \dot{m}_3 \cdot h_3 + \dot{m}_4 \cdot h_4 - \dot{m}_2 \cdot h_2 \tag{8}$$

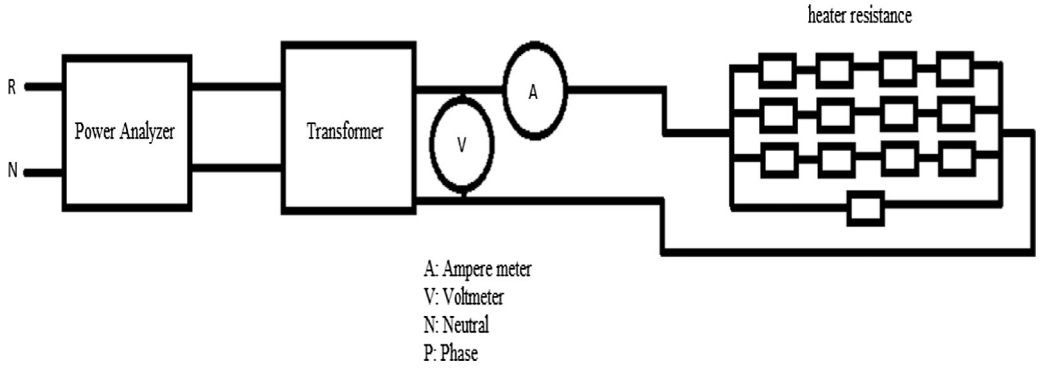

Fig. 5. The electrical diagram of electrical heater [31].

(a)

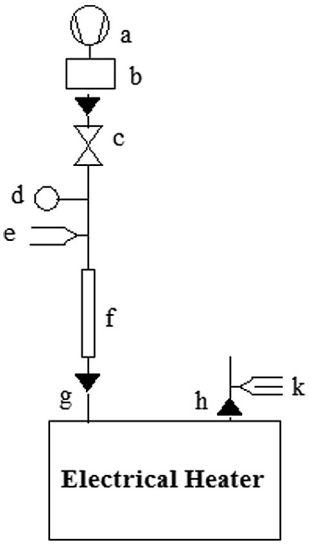

(b)

Fig. 6. The image (a) and schematic diagram (b) of the experimental set-up of the electrical heater [31].

Electrical heater;

$$\dot{W}_2 = \dot{m}_4 \cdot (h_5 - h_4) \tag{9}$$

and electrical power of electrical heater;

$$\dot{W}_{e,2} = \frac{\dot{m}_4 \cdot (h_5 - h_4)}{\eta_{eh}} \tag{10}$$

Dryer;

$$\dot{m}_{10} \cdot (h_{10} - h_{11}) = \dot{m}_7 \cdot c_{p,7} \cdot (T_8 - T_7) + (\dot{m}_7 - \dot{m}_8) \cdot h_{ss,8} \tag{11}$$

here, $c_{p,7}$: specific heat of tomato. The specific heat $(c_{p,tom})$ of tomato, calculated with Eq. (7) depending on temperature and constituents of tomato [40];

$$c_{p,tom} = c_{pro}X_{pro} + c_{fat}X_{fat} + c_{car}X_{car} + c_{fib}X_{fib} + c_{ash}X_{ash} + c_wX_w \tag{12}$$

here, X : the mass ratio of the food component. The mass composition ranges of tomato was given in Table 5.

The specific heat of the constituents of the product depending on temperature [40];

$$c_{pro} = 2.0082 + 1.2089 \cdot 10^{-3} \cdot T - 1.3129 \cdot 10^{-6} \cdot T^2 \tag{13}$$

$$c_{fat} = 1.9842 + 1.4733 \cdot 10^{-3} \cdot T - 4.8008 \cdot 10^{-6} \cdot T^2 \tag{14}$$

$$c_{car} = 1.5488 + 1.9625 \cdot 10^{-3} \cdot T - 5.9399 \cdot 10^{-6} \cdot T^2 \tag{15}$$

$$c_{fiber} = 1.8459 + 1.8306 \cdot 10^{-3} \cdot T - 4.6509 \cdot 10^{-6} \cdot T^2 \tag{16}$$

$$c_{ash} = 1.0926 + 1.8896 \cdot 10^{-3} \cdot T - 3.6817 \cdot 10^{-6} \cdot T^2 \tag{17}$$

$$c_w = 4.1289 - 9.0864 \cdot 10^{-5} \cdot T + 5.4731 \cdot 10^{-6} \cdot T^2 \tag{18}$$

According to energy analysis, the energy efficiency of RHVTAD system is obtained as following;

$$\eta_1 = \frac{\dot{m}_5 \cdot (h_5 - h_6)}{\dot{W}_{e,1} + \dot{W}_{e,2} + \dot{m}_1 \cdot h_1 + \dot{Q}_{RHVT} + \dot{m}_7 \cdot c_{p,7} \cdot T_7} \tag{19}$$

If the compressed air is obtained as a waste source from any process, the energy efficiency of system (RHVTADW) can be given by the following equation;

$$\eta_2 = \frac{\dot{m}_4 \cdot (h_4 - h_5)}{\dot{W}_{e,2} + \dot{m}_1 \cdot h_2 + \dot{Q}_{RHVT} + \dot{m}_7 \cdot c_{p,7} \cdot T_7} \tag{20}$$

If the drying without RHVT in which just the electrical heaters is used, then the energy efficiency of drying system (ED) is obtained as following;

$$\eta_3 = \frac{\dot{m}_5 \cdot (h_5 - h_6)}{\dot{W}_{e,2} + \dot{m}_1 \cdot h_1 + \dot{Q}_{RHVT} + \dot{m}_7 \cdot c_{p,7} \cdot T_7} \tag{21}$$

According to the assumptions, the governing exergy equations were obtained as given by Eqs. (22)–(33).Compressor;

$$\dot{E}x_{d,comp} = \dot{m}_1 \cdot \Psi_1 - \dot{m}_2 \cdot \Psi_2 + \dot{W}_{e,2} \tag{22}$$

RHVT;

$$\dot{E}x_{d,RHVT} = \dot{m}_2 \cdot \Psi_2 - (\dot{m}_3 \cdot \Psi_3 + \dot{m}_4 \cdot \Psi_4) + \dot{Q}_{RHVT} \cdot \left(\frac{T_o}{T_3} - 1\right) \tag{23}$$

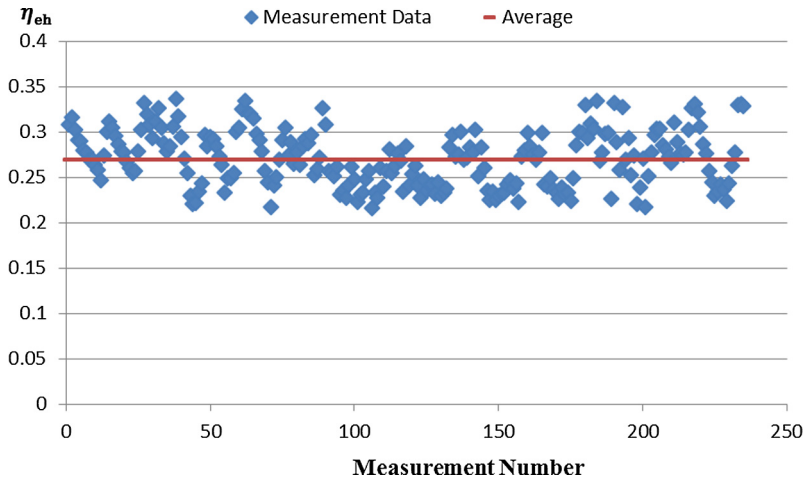

Fig. 7. The experimental results of the electrical heater efficiency [31].

Table 5
Mass composition ranges of tomato [40].

Constituents	% (X)
Water	93.76
Protein	0.85
Fat	0.33
Carbohydrate	3.54
Fiber	1.10
Ash	0.42

Electrical heater;

$$\dot{E}x_{d,eh} = \dot{m}_4 \cdot \Psi_4 - \dot{m}_5 \cdot \Psi_5 + \dot{W}_{e,2} \tag{24}$$

Dryer;

$$\dot{E}x_{d,dry} = \dot{m}_5 \cdot \Psi_5 + \dot{m}_7 \cdot \Psi_7 - (\dot{m}_6 \cdot \Psi_6 + \dot{m}_8 \cdot \Psi_8) \tag{25}$$

where Ψ indicates the specific exergy term and the specific exergy of the points in the RHVTAD system are given in Eqs. (18)–(25).

$$\begin{aligned}\Psi_1 = {} & [(c_p)_a + \omega_1 \cdot (c_p)_v] \cdot (T_1 - T_0) - T_0 \\ & \cdot \left[[(c_p)_a + \omega_1 \cdot (c_p)_v] \cdot \ln\left(\frac{T_1}{T_0}\right) - (R_a + \omega_1 \cdot R_v) \cdot \ln\left(\frac{P_1}{P_0}\right) \right] \\ & + T_0 \cdot \left[(R_a + \omega_1 \cdot R_v) \cdot \ln\left(\frac{1 + 1.6078 \cdot \omega_0}{1 + 1.6078 \cdot \omega_1}\right) \right. \\ & \left. + 1.6078 \cdot \omega_1 \cdot R_a \cdot \ln\left(\frac{\omega_1}{\omega_0}\right) \right]\end{aligned} \tag{26}$$

$$\Psi_2 = C_{p_2} \cdot \left[(T_2 - T_0) - T_0 \cdot \ln\frac{T_2}{T_0} \right] + R_a \cdot T_0 \cdot \ln\left(\frac{P_2}{P_0}\right) \tag{27}$$

$$\Psi_3 = c_{p_3} \cdot \left[(T_3 - T_0) - T_0 \cdot \ln\frac{T_3}{T_0} \right] + R_a \cdot T_0 \cdot \ln\left(\frac{P_3}{P_0}\right) \tag{28}$$

$$\begin{aligned}\Psi_4 = {} & [(c_p)_a + \omega_4 \cdot (c_p)_v] \cdot (T_4 - T_0) - T_0 \\ & \cdot \left[[(c_p)_a + \omega_4 \cdot (c_p)_v] \cdot \ln\left(\frac{T_4}{T_0}\right) - (R_a + \omega_4 \cdot R_v) \cdot \ln\left(\frac{P_4}{P_0}\right) \right] \\ & + T_0 \cdot \left[(R_a + \omega_4 \cdot R_v) \cdot \ln\left(\frac{1 + 1.6078 \cdot \omega_0}{1 + 1.6078 \cdot \omega_4}\right) \right. \\ & \left. + 1.6078 \cdot \omega_4 \cdot R_a \cdot \ln\left(\frac{\omega_4}{\omega_0}\right) \right]\end{aligned} \tag{29}$$

$$\begin{aligned}\Psi_5 = {} & [(c_p)_a + \omega_5 \cdot (c_p)_b] \cdot (T_5 - T_0) - T_0 \cdot \left[[(c_p)_a + \omega_5 \cdot (c_p)_b] \right. \\ & \left. \cdot \ln\left(\frac{T_5}{T_0}\right) - (R_a + \omega_5 \cdot R_v) \ln\left(\frac{P_5}{P_0}\right) \right] \\ & + T_0 \cdot \left[(R_a + \omega_5 \cdot R_v) \cdot \ln\left(\frac{1 + 1.6078 \cdot \omega_0}{1 + 1.6078 \cdot \omega_5}\right) \right. \\ & \left. + 1.6078 \cdot \omega_5 \cdot R_a \cdot \ln\left(\frac{\omega_5}{\omega_0}\right) \right]\end{aligned} \tag{30}$$

$$\begin{aligned}\Psi_6 = {} & [(c_p)_a + \omega_6 \cdot (c_p)_v] \cdot (T_6 - T_0) - T_0 \\ & \cdot \left[[(c_p)_a + \omega_6 \cdot (c_p)_v] \cdot \ln\left(\frac{T_6}{T_0}\right) - (R_a + \omega_6 \cdot R_v) \cdot \ln\left(\frac{P_6}{P_0}\right) \right] \\ & + T_0 \cdot \left[(R_a + \omega_6 \cdot R_v) \ln\left(\frac{1 + 1.6078 \cdot \omega_0}{1 + 1.6078 \cdot \omega_6}\right) \right. \\ & \left. + 1.6078 \cdot \omega_6 \cdot R_a \cdot \ln\left(\frac{\omega_6}{\omega_0}\right) \right]\end{aligned} \tag{31}$$

$$\Psi_7 = c_{p,7} \cdot \left[(T_7 - T_0) - T_0 \ln\frac{T_7}{T_0} \right] \tag{32}$$

$$\Psi_8 = c_{p,8} \cdot \left[(T_8 - T_0) - T_0 \cdot \ln\frac{T_8}{T_0} \right] \tag{33}$$

here, ω indicates the humidity ratio of air, reference dead state; $\omega^o = 0.02023$ [41]. In the system $v \cong v_\infty$ and the changing of pressure is neglected [42].

Exergetic efficiency of RHVTAD system;

$$\varepsilon_1 = 1 - \frac{\dot{E}x_{d,RHVT,comp} + \dot{E}x_{d,RHVT} + \dot{E}x_{d,eh} + \dot{E}x_{d,dry}}{\dot{m}_1 \cdot \Psi_1 + \dot{m}_7 \cdot \Psi_7 + \dot{W}_{e,1} + \dot{W}_{e,2} + \dot{Q}_{RHVT} \cdot \left(\frac{T_a}{T_3} - 1\right)} \tag{34}$$

Exergetic efficiency of RHVTADW system;

$$\varepsilon_2 = 1 - \frac{\dot{E}x_{d,comp} + \dot{E}x_{d,RHVT} + \dot{E}x_{d,eh} + \dot{E}x_{d,dry}}{\dot{m}_1 \cdot \Psi_2 + \dot{m}_7 \cdot \Psi_7 + \dot{W}_{e,2} + \dot{Q}_{RHVT} \cdot \left(\frac{T_a}{T_3} - 1\right)} \tag{35}$$

Exergetic efficiency of ED system;

$$\varepsilon_3 = 1 - \frac{\dot{E}x_{d,dry}}{\dot{m}_1 \cdot \Psi_1 + \dot{m}_7 \cdot \Psi_7 + \dot{W}_{e,2}} \tag{36}$$

4. Economic analysis

The life cycle cost (C_{sys}) of RHVTAD system occurs by the investment costs (C_{ic}), salvage cost (C_{sc}), operating costs (C_{OC}), maintenance costs (C_{mc}) and benefit (C_b).

$$C_{sys} = C_b - (C_{ic} + C_{sc} + C_{mc} + C_{OC}) \quad (37)$$

The salvage cost of RHVTAD system (Eq. (33)) was taken as 10% of the investment cost [43].

$$C_{sc} = C_{ic} \cdot 0.10 \quad (38)$$

The maintenance cost of RHVTAD system (Eq. (34)) was taken as 2% of the investment cost of the RHVTAD system [43,44].

$$C_{mc} = C_{ic} \cdot 0.02 \quad (39)$$

The benefit of RHVTAD system (Eq. (35)) includes dried tomatoes earning.

$$C_b = (\dot{m}_{8,33} \cdot t_{33} \cdot 3600 + \dot{m}_{8,16} \cdot t_{16} \cdot 3600) \cdot 15.66 \quad (40)$$

where t_{33}; summer period (h), t_{16}; winter period (h), $\dot{m}_{8,33}$; mass of dried tomato summer period (kg/s) and $\dot{m}_{8,16}$; mass of dried tomato winter period (kg/s). The unit price of dried tomato is 15.66 €/kg [45–47].

Operating costs of the system;

$$C_{OC} = C_e + C_{fp} \quad (41)$$

where C_e; electrical costs of the RHVTAD system and C_{fp}; fresh tomato costs. Electrical costs;

$$C_e = ((\dot{W}_{e,1,33} + \dot{W}_{e,2,33}) \cdot t_{33}) + ((\dot{W}_{e,1,16} + \dot{W}_{e,2,16}) \cdot t_{16}) \cdot 0.107 \quad (42)$$

where 0.107 €/kWh is the electrical energy cost [48].

The fresh product costs;

$$C_{fp} = \frac{((\dot{m}_{12,33} \cdot t_{33}) + (\dot{m}_{12,16} \cdot t_{16}))}{t_k} \cdot 0.6 \quad (43)$$

where $\dot{m}_{8,33}$; mass of the fresh tomato summer period, $\dot{m}_{7,16}$; mass of the fresh tomato winter period and 0.6 €/kg is the cost of fresh tomato [49].The net cash flow;

$$C_T = (C_b - C_{OC} - C_{mc}) \cdot (1+i)^{t-1} \quad (44)$$

in this equation, i; the interest rate and t; the related year time of cash flow.

here, i; the interest rate and t; the related year time of cash flow. The Net Present Value (NPV) of RHVTAD system (Eq. (40));

$$NPV = (C_{sc} - C_{ic}) + \sum_{t=0}^{ol} \frac{C_T}{(1+j)^t} \quad (45)$$

where ol; the lifetime of RHVTAD system, j; the discount rate. In this study, the lifetime of RHVTAD system was added to calculations as 20 years. The discount and interest rates were taken as 9% and 7.25%, respectively [50,51].

5. Results and discussion

The change in energy, exergy efficiency, and NPV according to parameters discussed in each chart within the other RHVT parameters and operating conditions indicates the same trend. So the most effective parameters graphs are used in the study according to analyzes. The RHVT designs with the temperature differences of the hot stream and inlet stream of RHVT of higher than 5 K were used in the RHVTAD system. For this reason, some parameters had limited in these graphs. Handling the operating parameters as T_1 = 306.15 K, T_5 = 328.15 K, T_6 = 308.15 K, h/w = 0.44, d/D = 0.51, α = 30°, 3rd control valve position, the variation of energy efficiency of the RHVTAD system with different inlet air pressure of RHVT (P_2) and RHVT body was obtained as seen in Fig. 8.

According to Fig. 8, the energy efficiency (η_1) values of RHVTAD system increase with the increase of L/D, accept one design in which the P_2 at 201.325 kPa. The energy efficiency of the system increased by the decrease of the inlet stream pressure of RHVT (P_2). The energy efficiency of proposed RHVTAD system ranges between 0.0468 and 0.0330. The changing of energy efficiency values of RHVTAD system for T_1 = 306.15 K, T_5 = 328.15 K, P_2 = 601.325 kPa, h/w = 0.44, d/D = 0.51, L/D = 40, according to different control valve angle (α) and control valve opening position are given in Fig. 9.

As seen in Fig. 9, the highest energy efficiency of RHVTAD system was obtained at the 3rd control valve opening position when the control valve angle was changed between 45° and 60°. However, for the 30° of the control valve angle, the highest energy efficiency value calculated for the 4th opening position. The highest energy efficiency value of RHVTAD system was obtained as 0.0362 for 3rd control valve opening position and 60° of the control valve angle. The changing of the energy efficiency values of RHVTAD system for T_1 = 306.15 K, T_5 = 328.15 K, T_6 = 308.15 K, P_2 = 601.325 kPa, L/D = 17.5, 30° of control valve angle, 3rd control valve position according to different RHVT generator (h/w, d/D) are given in Fig. 10.

As seen in Fig. 10, the highest energy efficiency value of RHVTAD system was obtained as 0.0330 for h/w = 0.44, d/D = 0.51 (C type RHVT generator). When h/w was kept constant at 0.25, the energy efficiency of the system increase by the decrease of d/D. The energy efficiency of proposed RHVTAD system ranges between 0.0296 and 0.0330. The changing of the energy efficiency of RHVTAD system for T_1 = 306.15 K, h/w = 0.44, d/D = 0.51, P_2 = 601.325 kPa, L/D = 40, α = 30°, 3rd control valve position according to different inlet temperature of dryer air and (T_5) and differences of inlet and outlet temperature (ΔT_{5-6}) of dryer air are given in Fig. 11.

According to Fig. 11, the energy efficiency of RHVTAD system increase with the increase of inlet air temperature of the dryer up to 333.15 K and the increase of the differences of inlet and outlet air temperature of the dryer. At this stage, the energy efficiency of proposed RHVTAD system ranges between 0.0033 and 0.0348. The change of energy efficiency of RHVTAD system for T_5 = 328.15 K, T_6 = 308.15 K, h/w = 0.44, d/D = 0.51, P_2 = 601.325 kPa, L/D = 40, 30° of control valve angle, 3rd control valve position according to different drying system designs and ambient air temperature are given in Fig. 12.

As seen in Fig. 12, the maximum energy efficiency of the system was calculated as 0.0545 and 0.0508 for the RHVTADW system at 306.15 K and 289.15 K of ambient temperature, respectively.

The usage of the operating parameters as T_1 = 306.15 K, T_5 = 328.15 K, T_6 = 308.15 K, h/w = 0.44, d/D = 0.51, 30° of control valve angle, 3rd control valve position, the variation of exergy efficiency of the RHVTAD system with different inlet air pressure of RHVT (P_2) and RHVT body was obtained as seen in Fig. 13.

As seen in Fig. 13, the exergy efficiency (ε_1) values of RHVTAD system increase by the decrease of the ratio of L to D (decrease of the RHVT body length) when the P_2 was kept constant. The exergy efficiency of proposed RHVTAD system ranges between 0.0010 and 0.0027. The changing of exergy efficiency values of RHVTAD system for T_1 = 306.15 K, T_5 = 328.15 K, P_2 = 601.325 kPa, h/w = 0.44, d/D = 0.51, and L/D = 40, according to different control valve angle (α) and control valve opening position are given in Fig. 14.

As seen in Fig. 14, the exergy efficiency of RHVTAD system highest value was obtained at the 2nd control valve opening position when α was changed between 45° and 60°. But for the 30° of the control valve angle was kept constant, the highest exergy efficiency value calculated for the 4th opening position. The highest exergy efficiency value of RHVTAD system was obtained as 0.0031 for 2nd control valve opening position and 60° of the control valve angle. The change of exergy efficiency values of RHVTAD system for T_1 = 306.15 K, T_5 = 328.15 K, T_6 = 308.15 K, P_2 = 601.325 kPa,

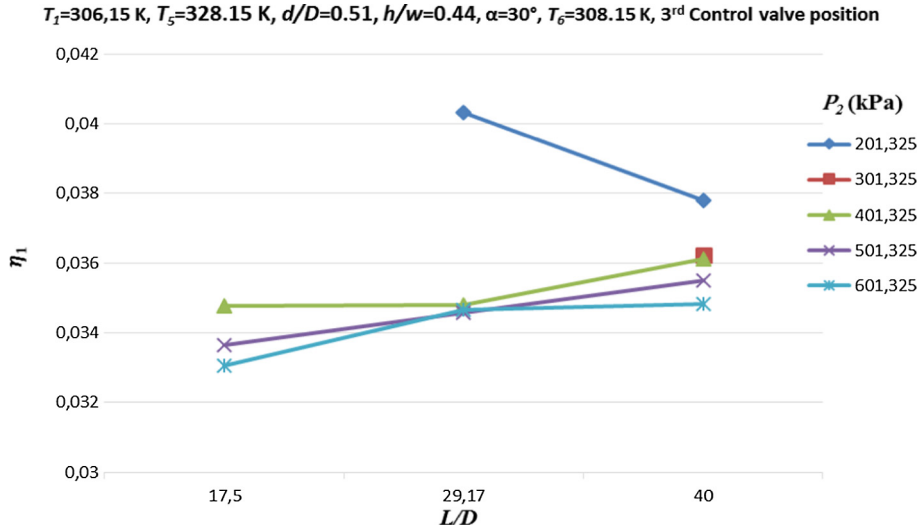

Fig. 8. The variation of η_1 versus P_2 and RHVT body.

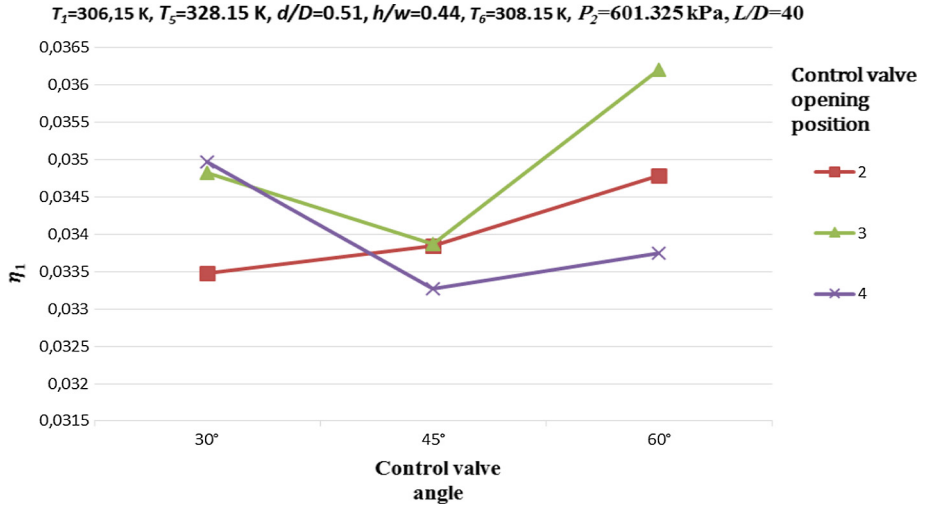

Fig. 9. The variation of η_1 versus control valve opening position and control valve angle.

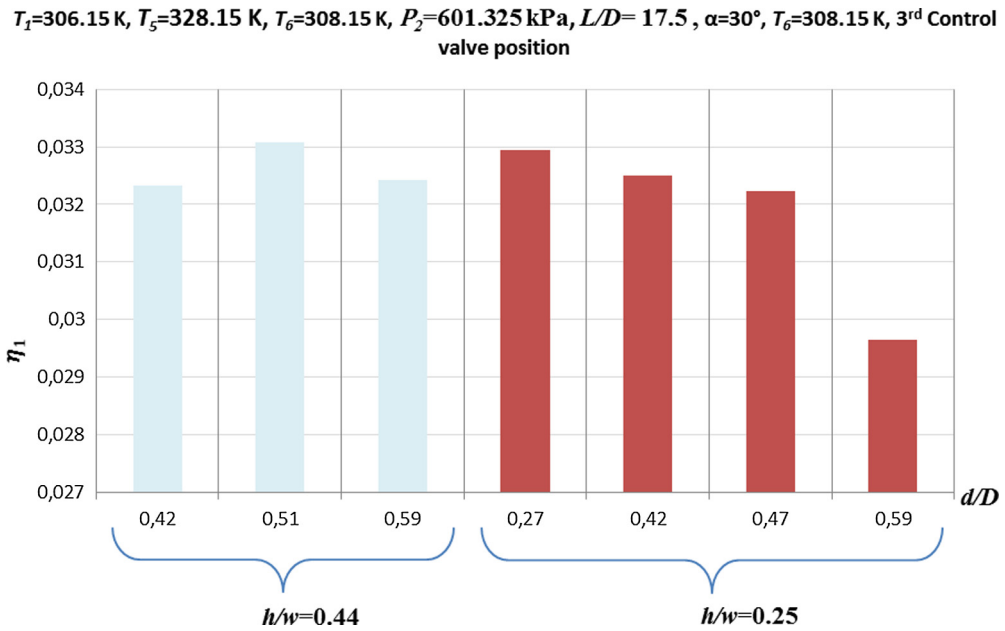

Fig. 10. The variation of η_1 versus RHVT generator.

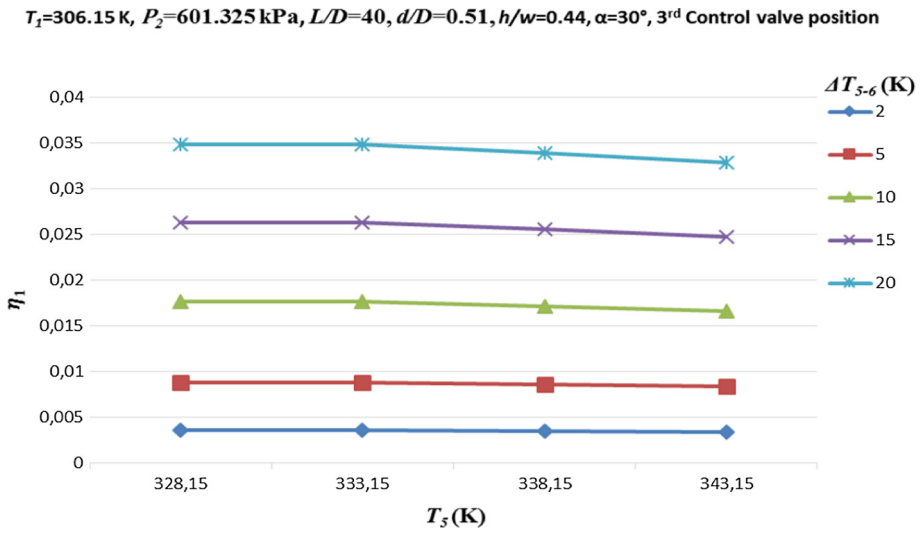

Fig. 11. The variation of η_1 versus ΔT_{5-6} and T_5.

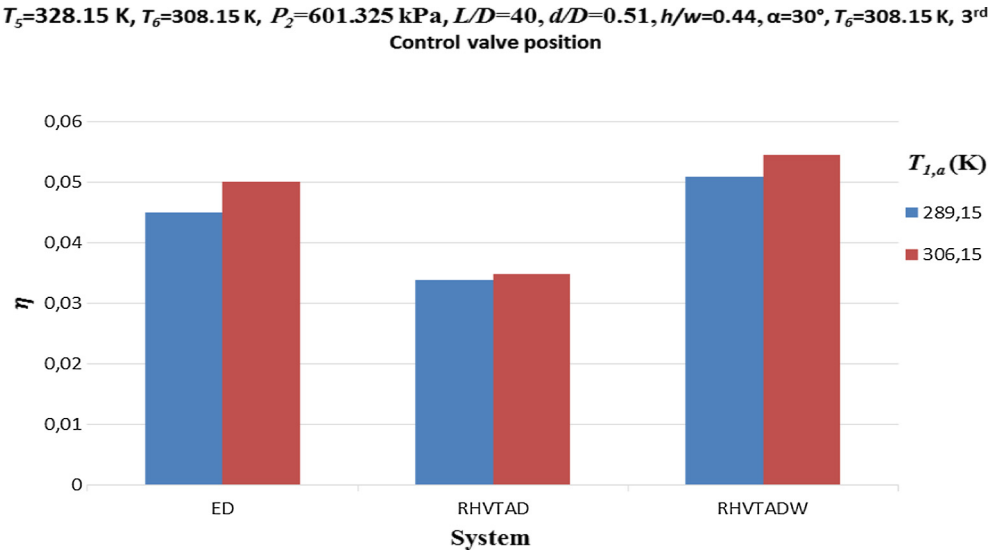

Fig. 12. The variation of η_1 versus system designs and $T_{1,a}$.

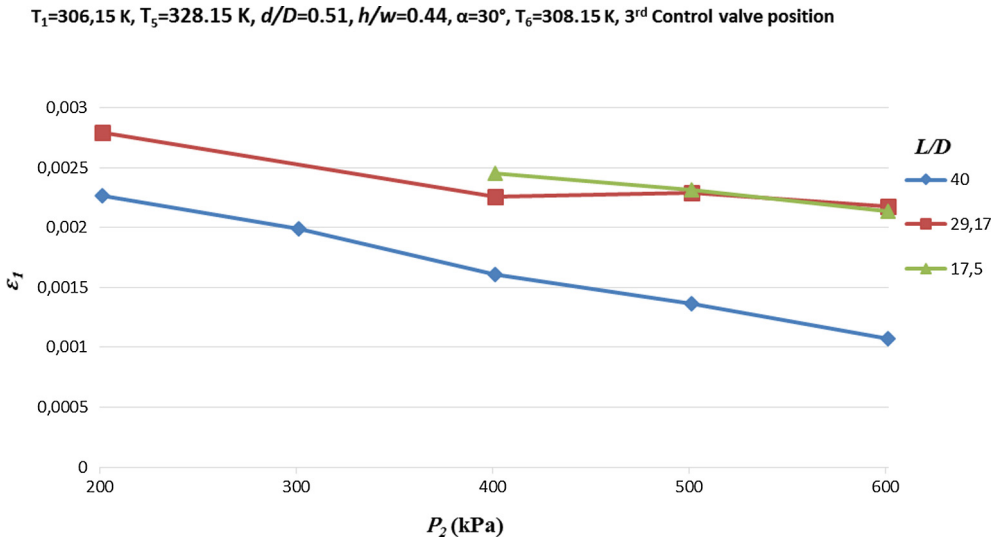

Fig. 13. The variation of ε_1 versus P_2 and RHVT body.

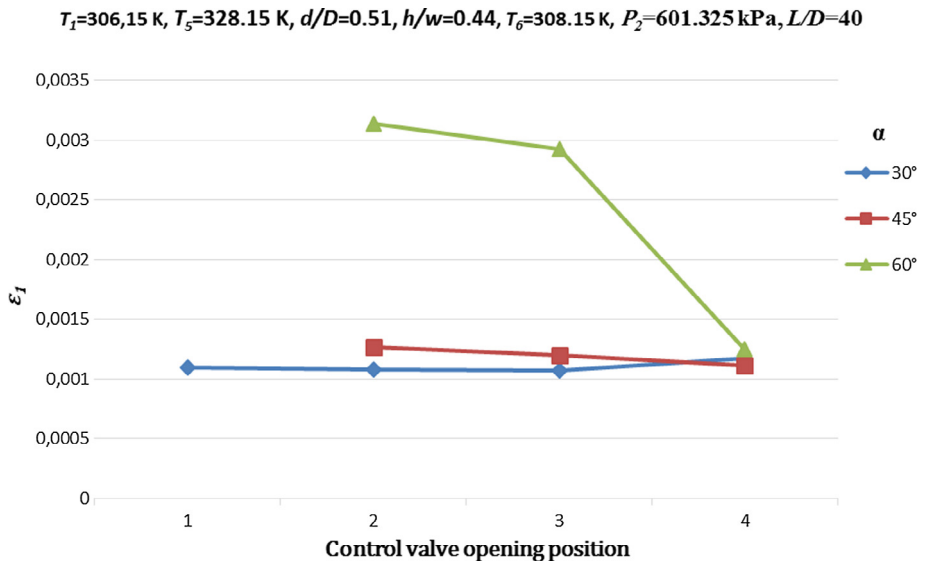

Fig. 14. The variation of ε_1 versus control valve opening position and control valve angle.

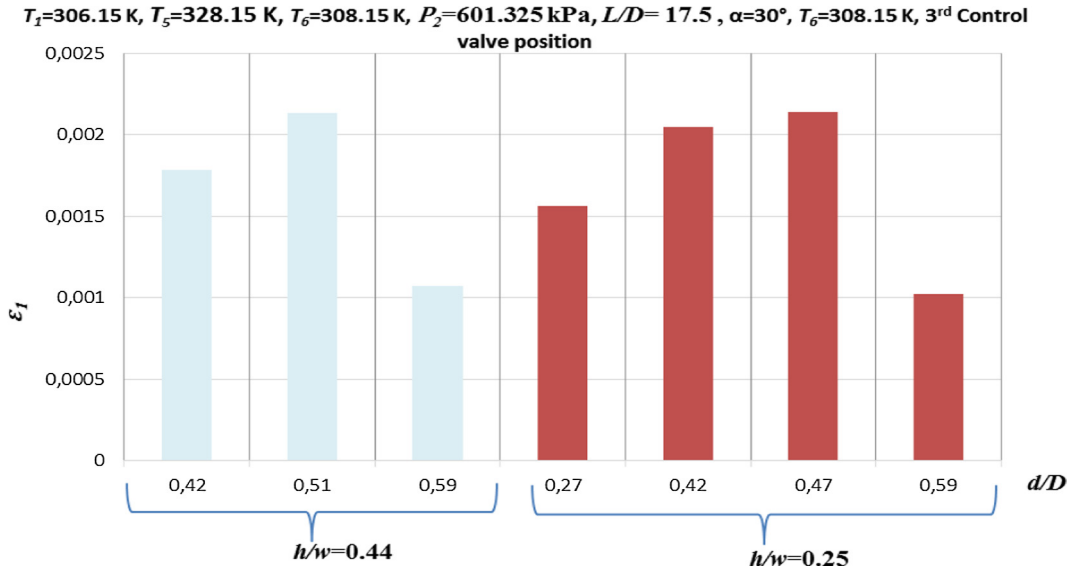

Fig. 15. The variation of ε_1 versus RHVT generator.

L/D = 17.5, 30° of control valve angle, 3rd control valve position according to different RHVT generator are given in Fig. 15.

As seen in Fig. 15, the highest exergy efficiency value of RHVTAD system was obtained as 0.00214 for h/w = 0.25, d/D = 0.47 (O type RHVT generator). When the h/w was kept constant at 0.42 and 0.59, the exergy efficiency of the system increased by the increase of d/D. The exergy efficiency of proposed RHVTAD system ranges between 0.0010 and 0.00214. The change of exergy efficiency of RHVTAD system for T_1 = 306.15 K, h/w = 0.44, d/D = 0.51, L/D = 40, P_2 = 601.325 kPa, α = 30°, 3rd control valve position according to different T_5 and ΔT_{5-6} are given in Fig. 16.

According to Fig. 16, the exergy efficiency of RHVTAD system increase with the increase of inlet air temperature of the dryer and the decrease of the differences of inlet and outlet air temperature of the dryer. At this stage, the exergy efficiency of proposed RHVTAD system ranges between 0.0010 and 0.0136. The changing of exergy efficiency value of RHVTAD system for T_5 = 328.15 K, T_6 = 308.15 K, h/w = 0.44, d/D = 0.51, L/D = 40, P_2 = 601.325 kPa, 30° of control valve angle, 3rd control valve position according to different drying system designs and ambient air temperature are given in Fig. 17.

As seen in Fig. 17, the maximum exergy efficiency of the drying system was calculated as 0.0027 for the RHVTADW system at 289.15 K of ambient temperature and the highest exergy efficiency determined as 0.0020 for ED system at 306.15 K of ambient temperature.

The utilization of the operating parameters as T_1 = 306.15 K, T_5 = 328.15 K, T_6 = 308.15 K, h/w = 0.44, d/D = 0.51, 30° of control valve angle, 3rd control valve position, the variation of *NPV* of the RHVTAD system with different inlet air pressure of RHVT (P_2) and RHVT body was obtained as seen in Fig. 18.

As seen in Fig. 18, the *NPV* values of RHVTAD system increase by the increase of L/D when P_2 is kept constant. The *NPV* values of RHVTAD system increase by the decrease of the inlet stream pressure of RHVT (P_2) when L/D = 40. The *NPV* of proposed RHVTAD

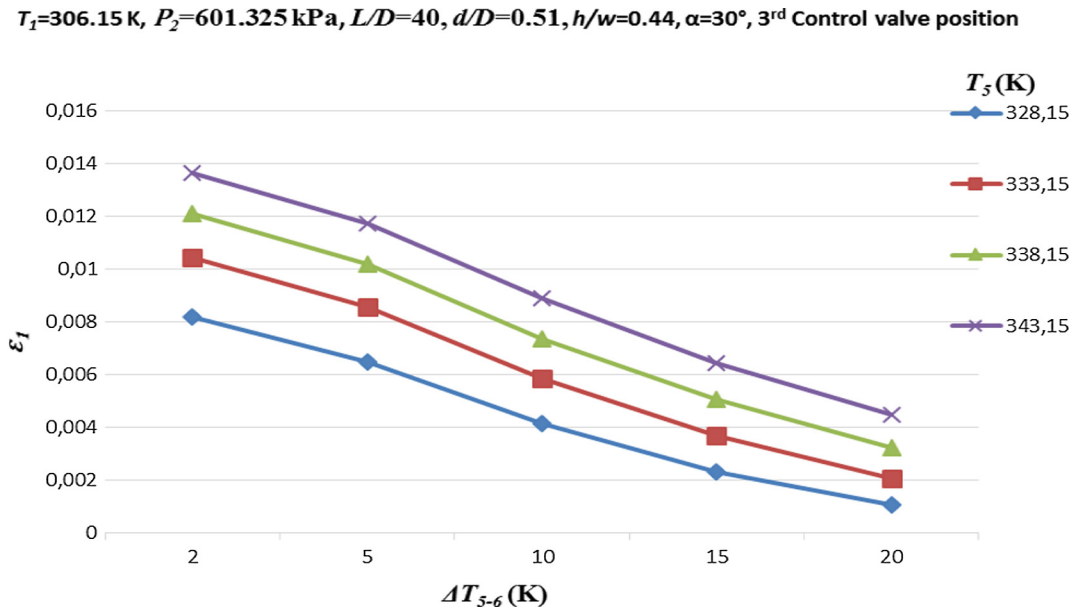

Fig. 16. The variation of ε_1 versus ΔT_{5-6} and T_5.

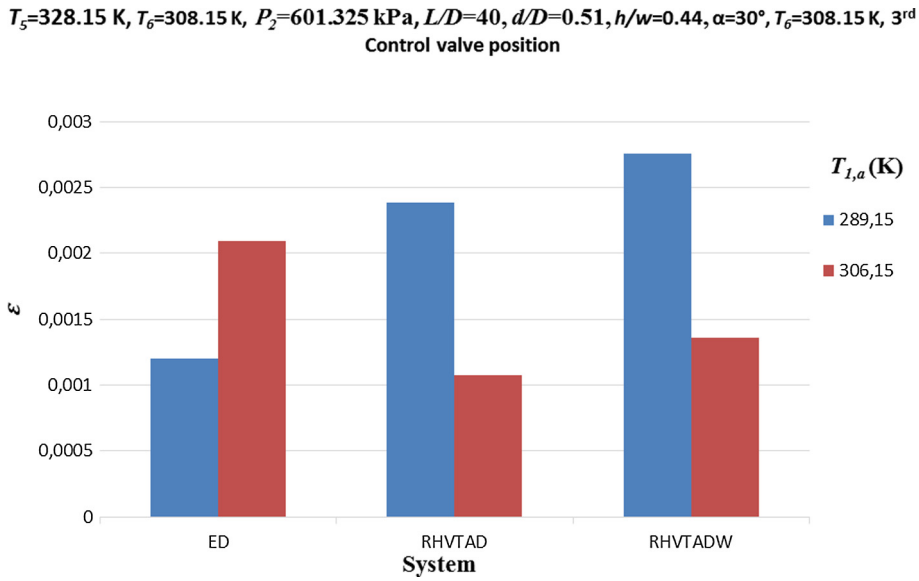

Fig. 17. The variation of ε versus systems designs and $T_{1,a}$.

system ranges between −29018.90 € and 23707.08 €. The changing of *NPV* values of RHVTAD system for T_1 = 306.15 K, T_5 = 328.15 K, P_2 = 601.325 kPa, h/w = 0.44, d/D = 0.51 and L/D = 40, according to different control valve angle (α) and control valve opening position are given in Fig. 19.

As seen in Fig. 19, the highest value of *NPV* of RHVTAD system was obtained at the 3rd control valve opening position when the control valve angle was kept constant at 60° and 30°. But for the 45° of the control valve angle was kept constant, the highest *NPV* value calculated for the 2nd opening position. The highest *NPV* value of RHVTAD system was obtained as 23707.08 € for 3rd control valve opening position and 30° of the control valve angle. The change of *NPV* values of RHVTAD system for T_1 = 306.15 K, T_5 = 328.15 K, T_6 = 308.15 K, P_2 = 601.325 kPa, L/D = 17.5, 30° of control valve angle, 3rd control valve position according to different RHVT generator are given in Fig. 20.

As seen in Fig. 20, the highest *NPV* value of RHVTAD system was obtained as −22922.70 € for h/w = 0.44, d/D = 0.59 (D type RHVT generator). The exergy efficiency of proposed RHVTAD system ranges between −41116.80 € and -22922.70 €. The change of *NPV* of RHVTAD system for T_1 = 306.15 K, h/w = 0.44, d/D = 0.51 and L/D = 40, P_2 = 601.325 kPa, α = 30°, 3rd control valve position according to different T_5 and ΔT_{5-6} are given in Fig. 21.

According to Fig. 21, the *NPV* of RHVTAD system increase with the decrease of inlet air temperature of the dryer and the increase of differences between inlet and outlet air temperature. At this stage, the *NPV* of proposed RHVTAD system ranges between −206446.00 € and 23712.24 €. The change of *NPV* of RHVTAD system for T_5 = 328.15 K, T_6 = 308.15 K, h/w = 0.44, d/D = 0.51 and L/D = 40, P_2 = 601.325 kPa, 30° of control valve angle, 3rd control valve position according to different drying system designs are given in Fig. 22.

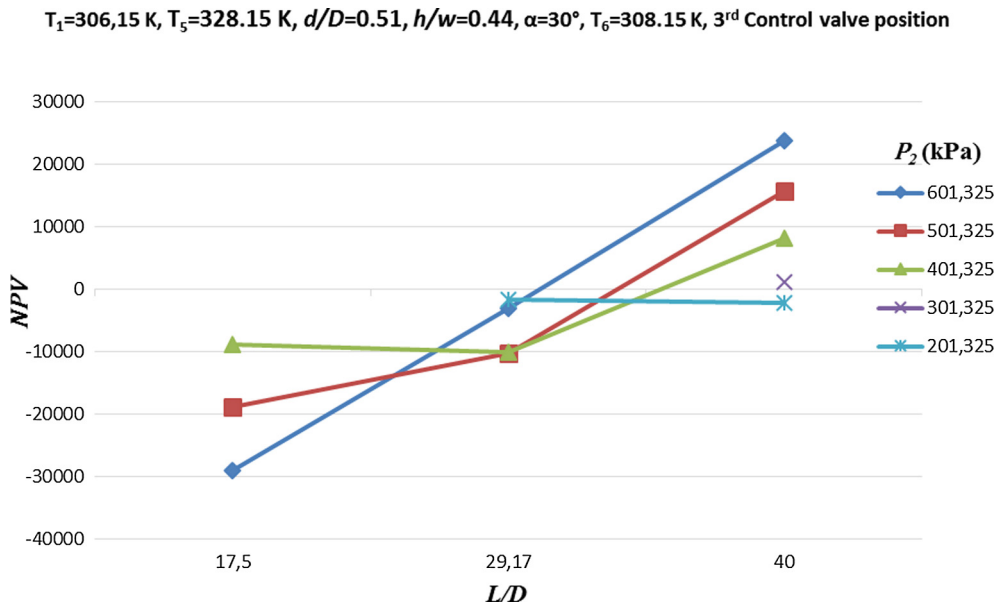

Fig. 18. The variation of *NPV* versus P_2 and RHVT body.

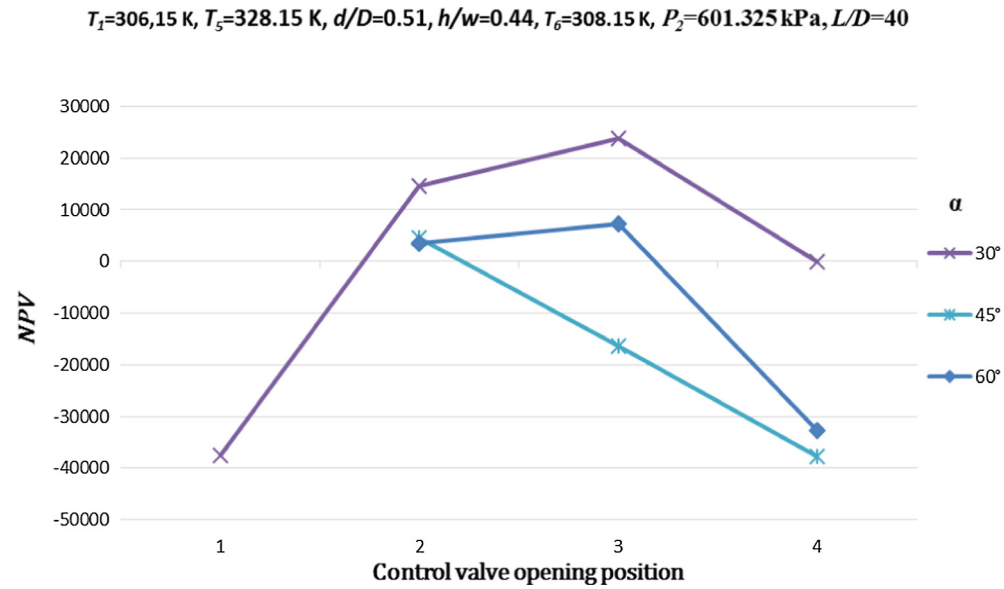

Fig. 19. The variation of *NPV* versus control valve opening position and control valve angle.

As seen in Fig. 22, the maximum *NPV* of the drying system was calculated as 182253.70 € for RHVTADW system. At this stage, the *NPV* of proposed RHVTAD and ED system were determined as 23712.24 € and 177847.80 €, respectively.

The energy and exergy efficiencies of RHVTAD system increase with the increase of the inlet stream temperature of dryer, the control valve angle and the decrease of the inlet stream pressure of RHVT. The energy efficiency of the RHVTAD system increase with the increase of *L*/*D*. The increase of the temperature differences of inlet and outlet dryer air cause to the increase of energy efficiency and the decrease of exergy efficiency. The increase in the ambient temperature causes to increase the exergy efficiency and the decrease of energy efficiency. But the same results were not observed according to *NPV*. The *NPV* of the RHVTAD system increased with the increase of the inlet stream pressure of RHVT, the temperature differences of inlet and outlet dryer air, *L*/*D* and the decrease of the inlet temperature of the dryer. The highest *NPV* value of the RHVTAD system was obtained for 30° control valve angle and 3rd control valve opening position. It was found that the effect of *h*/*w* on energy efficiency, exergy efficiency, and *NPV* was negligible.

According to the energy analysis results, the most effective *L*/*D*, *h*/*w*, *d*/*D*, control valve angle and control valve opening position were determined as 40, 0.44, 0.51, 60° and 3rd respectively. The maximum energy efficiency of RHVTAD system was determined as 0.0370 at 306.15 K of ambient temperature. These system properties were T_5 of 328.15 K, T_6 of 308.15 K and P_2 of 401.325 kPa. For the same operating conditions, the energy efficiency of the RHVTAD was obtained as 0.0346 at 289.15 K. Exergy efficiency of this system was calculated as 0.0017 and 0.0025 for the summer mode and winter mode, respectively. *NPV* of this RHVTAD system was calculated as 2953.99 €. For the same operating conditions,

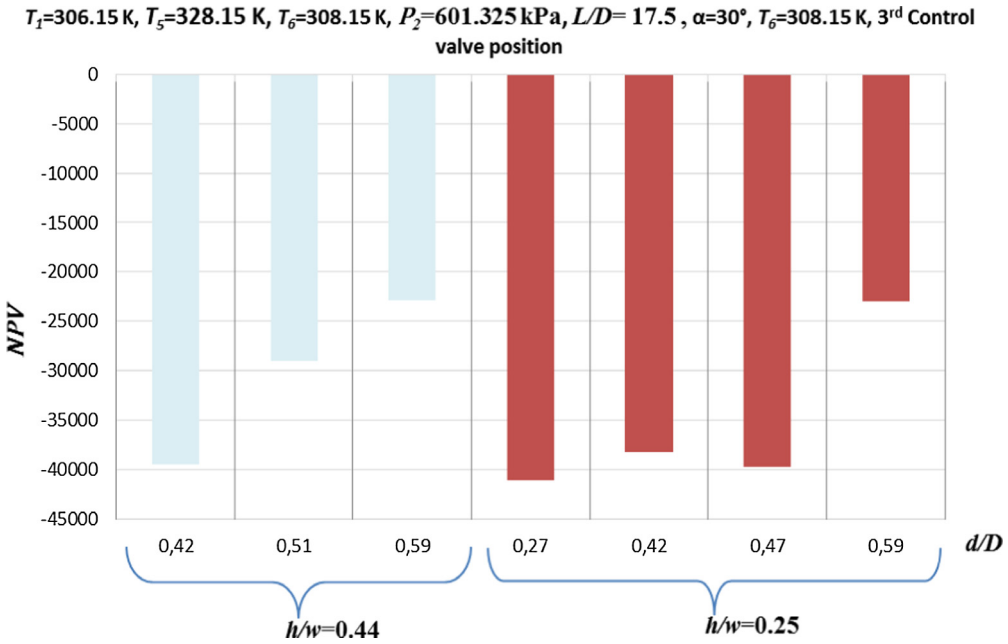

Fig. 20. The variation of *NPV* versus RHVT generator.

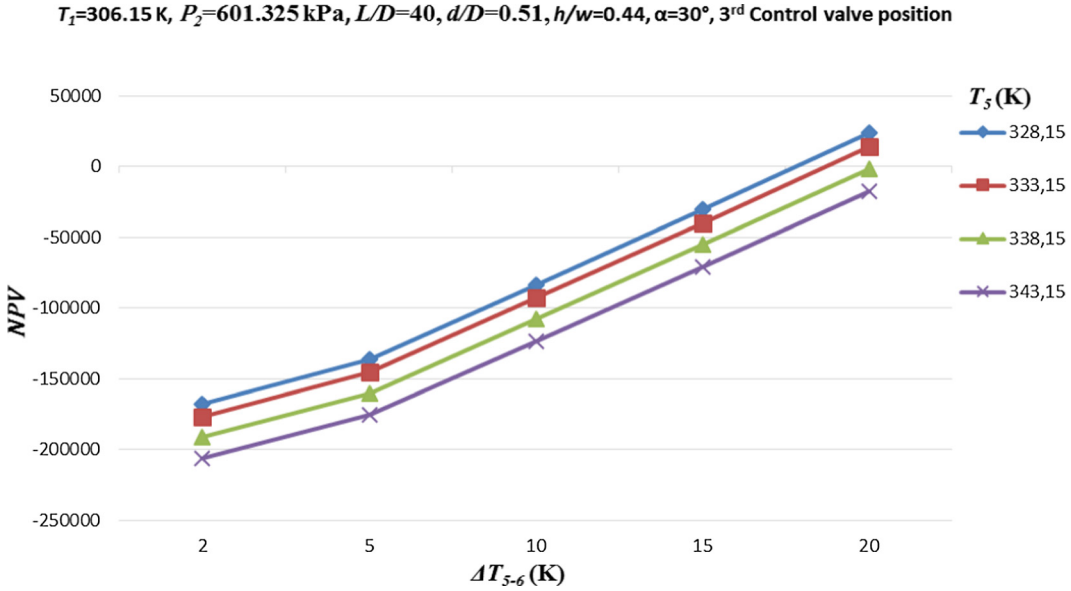

Fig. 21. The variation of *NPV* versus ΔT_{5-6} and T_5.

the energy efficiency of the ED system was calculated as 0.0500 and 0.0449 at 306.15 K and 289.15 K of ambient temperature, respectively. The energy efficiency of RHVTADW system is determined as 0.0527 and 0.0470 for the summer mode and winter mode, respectively. For the same operating conditions and RHVT geometries, the best energy efficiency was obtained for the RHVTADW system which is used waste air for inlet stream of RHVT.

According to the exergy analysis results, the most effective L/D, h/w, d/D, control valve angle and control valve opening position were determined as 40, 0.44, 0.51, 30° and 3rd, respectively. The maximum exergy efficiency of RHVTAD system was determined as 0.0033 at 289.15 K of ambient temperature. These system properties were T_5 of 333.15 K, T_6 of 313.15 K and P_2 of 501.325 kPa. For the same operating conditions, the exergy efficiency of the RHVTAD was obtained as 0.0023 at 306.15 K. Energy efficiency of this system was 0.0348 and 0.0327 for the summer mode and winter mode, respectively. *NPV* of this RHVTAD system was calculated as 3138.47 €. For the same operating conditions, exergy efficiency of the ED system was calculated as 0.00376 and 0.0023 at 306.15 K and 289.15 K of ambient temperature, respectively. The exergy efficiency of RHVTADW system is determined as 0.0028 and 0.00377 for the summer mode and winter mode, respectively. For the same operating conditions and RHVT geometries, the best exergy efficiency was obtained for the RHVTADW system which is used waste air for inlet stream of RHVT.

According to the economic analysis results, the most effective L/D, h/w, d/D, control valve angle and control valve opening position are 40, 0.44, 0.51, 30° and 3rd respectively. The maximum *NPV* of RHVTAD system was determined as 23711.88 €. These system properties were T_5 of 328.15 K, T_6 of 308.15 K and P_2 of 601.325 kPa. Under the same conditions, the energy efficiency of

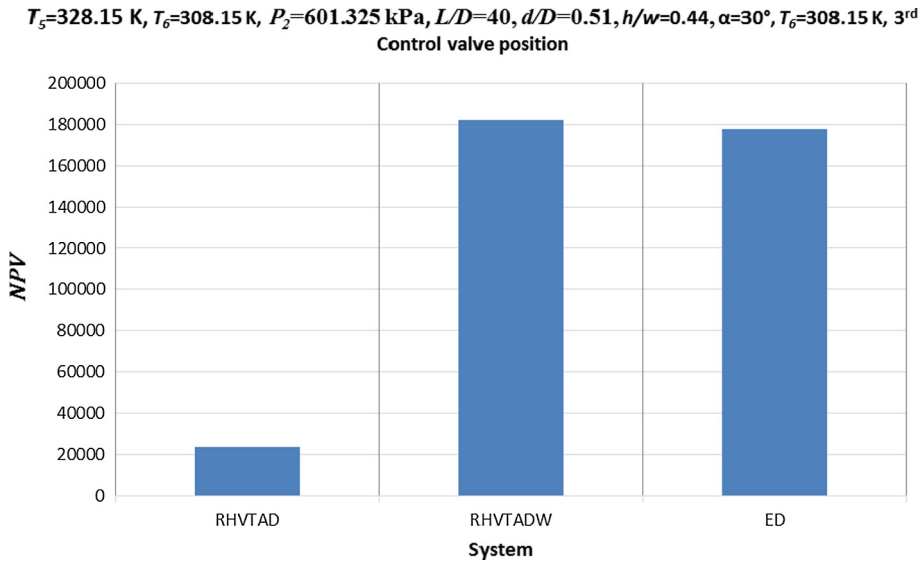

Fig. 22. The variation of versus *NPV* system designs.

the RHVTAD system was calculated as 0.0348 and 0.0338 for the summer mode and winter mode, respectively. Exergy efficiency of this system was 0.0010 and 0.0023 for the summer mode and winter mode, respectively. For the same operating conditions, the energy efficiency of the ED system was calculated as 0.0500 and 0.0449 at 306.15 K and 289.15 K, respectively. The energy efficiency of RHVTADW system is determined as 0.0545 and 0.0508 for the summer mode and winter mode, respectively. Under the same operating conditions, the *NPV* of the ED system and RHVTADW system were calculated as 177847.80 € and 182253.70 €.

6. Conclusion

In this study, the performance of electrical drying system integrated with Ranque-Hilsch vortex tube (RHVTAD) was investigated. For this purpose, the geometrical parameters, inlet and outlet temperatures of the dryer, the pressure of inlet flow of RHVT and the cold mass fraction were taken into account. Additionally, 8 different the helical vortex generators, 3 different control valve angles and 3 different RHVT bodies were also taken into consideration.

The same operating conditions of drying system and RHVT geometries, the best *NPV* was obtained for the RHVTADW system which is used waste air for inlet stream of RHVT. The best performance of the RHVTAD system determined for L/D = 40, h/w = 0.44, d/D = 0.51, control valve angle of 30°, 3rd control valve opening position, T_5 of 328.15 K, T_6 of 308.15 K and P_2 of 601.325 kPa.

As a result of the thermodynamic and NPV analysis, it is determined that the RHVTAD system is worth to invest. Considering the results, if pressurized air obtained from the exhaust of any system as a waste stream, the RHVTADW system is more economical than the electrical drying system. The cold stream of vortex tube wasn't addressed in this study. So, a hybrid system in which both the cold and hot streams of RHVT were used would be more effective from the thermodynamic and economic points of view. So, it is strongly advised to study the design of a hybrid system in which RHVT's cold and hot outlet flow are used together.

Acknowledgement

This study was supported by Scientific Research Projects Unit of Dumlupinar University (DPUBAP) with the project no of 2013/5.

References

[1] G.J. Ranque, Expériences sur la détente giratoire avec productions simultanées d'un échappement d'air chaud et d'un échappement d'air froid, Journal de Physique et Le Radium (in French) 7 (4) (1933) 112–114.
[2] R. Hilsch, The use of expansion of gases in a centrifugal field as a cooling process, Rev. Sci. Instrum. 18 (2) (1947) 108–113.
[3] J. Lewins, A. Bejan, Vortex tube optimization theory, Energy 24 (1998) 931–943.
[4] T.T. Cockerill, Thermodynamics and Fluid Mechanics of a Ranque–Hilsch Vortex Tube (MSc Thesis), University of Cambridge, 1998.
[5] M.H. Saidi, M.S. Valipour, Experimental modeling of vortex tube refrigerator, Appl. Therm. Eng. 23 (2003) 1971–1980.
[6] N. Pourmahmoud, A. Hassanzadeh, O. Moutaby, Numerical analysis of the effect of helical nozzles gap on the cooling capacity of Ranque-Hilsch vortex tube, Int. J. Refrig. 35 (2012) 1473–1483.
[7] M.R. Andalibi, S.H. Azizi, P. Mohajeri Khameneh, M. Janmohammadi, Effect of diameter and diameter of orifice on the performance of vortex tube, Int. J. Sci. Eng. Invest. 1 (2) (2012) 89–93.
[8] K. Chang, Q. Li, G. Zhou, Q. Li, Experimental investigation of vortex tube refrigerator with a divergent hot tube, Int. J. Refrig. 34 (2011) 322–327.
[9] T. Dutta, K.P. Sinhamahapatra, S.S. Bandyopadhyay, Numerical investigation of gas species and energy separation in the Ranque-Hilsch vortex tube using real gas model, Int. J. Refrig. 34 (2011) 2118–2128.
[10] Y. Xue, M. Arjomandi, R. Kelso, Visualization of the flow structure in a vortex tube, Exp. Therm. Fluid Sci. 35 (2011) 1514–1521.
[11] N. Rahbar, M. Taherian, M. Shateri, M.S. Valipour, Numerical investigation on flow behavior and energy separation in a micro scale vortex tube, Therm. Sci. 19 (2) (2015) 619–630.
[12] W. Fröhlingsdorf, H. Unger, Numerical investigations of the compressible flow and the energy separation in the Ranque-Hilsch vortex tube, Int. J. Heat Mass Transfer 31 (1998) 304–311.
[13] S. Eiamsa-ard, P. Promvonge, Numerical investigation of the thermal separation in a Ranque-Hilsch vortex tube, Int. J. Heat Mass Transfer 50 (5–6) (2007) 821–832.
[14] U. Behera, P.J. Paul, S. Kasthurirengan, R. Karunanithi, S.N. Ram, K. Dinesh, S. Jacob, CFD analysis and experimental investigations towards optimizing the parameters of Ranque-Hilsch vortex tube, Int. J. Heat Mass Transfer 48 (2005) 1961–1973.
[15] N.F. Aljuwayhel, G.F. Nellis, S.A. Klein, Parametric and internal study of the vortex tube using a CFD model, Int. J. Refrig. 28 (2005) 442–450.
[16] S. Eiamsa-ard, Experimental investigation of energy separation in a counter-flow Ranque-Hilsch vortex tube with multiple inlet snail entries, Int. Commun. Heat Mass Transfer 37 (2010) 637–643.
[17] S. Eiamsa-ard, K. Wongcharee, P. Promvonge, Experimental investigation on energy separation in a counter-flow Ranque-Hilsch vortex tube: effect of cooling a hot tube, Int. Commun. Heat Mass Transfer 37 (2010) 156–162.
[18] V. Kırmacı, Exergy analysis and performance of a counter flow Ranque-Hilsch vortex tube having various nozzle numbers at different inlet pressures of oxygen and air, Int. J. Refrig. 32 (2009) 1626–1633.
[19] K. Dincer, Y. Yılmaz, A. Berber, S. Baskaya, Experimental ınvestigation of performance of hot cascade thype Ranque-Hilsch vortex tube and exergy analysis, Int. J. Refrig. 34 (2011) 1117–1124.
[20] E.C. Lecumberri, J.M.S. Lizarraga, Mass, energy, entropy and exergy rate balance in a Ranque-Hilsch vortex tube, J. Technol. Sci. Educ. 3 (3) (2013) 122–132. http://upcommons.upc.edu/bitstream/handle/2099/16320/86-588-1-PB.pdf.

[21] Y. Xue, M. Arjomandi, R. Kelso, Energy analysis with in a vortex tube, Exp. Therm. Fluid Sci. 52 (2014) 139–145.
[22] I. Cebeci, V. Kırmacı, U. Topcuoglu, The effects of orifice nozzle number and nozzle made of polyamide plastic and aluminum with different inlet pressures on heating and cooling performance of counter flow ranque-hilsch vortex tubes: an experimental investigation, Int. J. Refrig. (2016) (in press), Accepted Manuscript, http://dx.doi.org/10.1016/j.ijrefrig.2016.07.013.
[23] K. Dincer, S. Tasdemir, S. Baskaya, B.Z. Uysal, Modeling of the effects of length to diameter ratio and nozzle number on the performance of counterflow Ranque-Hilsch vortex tubes using artificial neural networks, J. Appl. Therm. Eng. 28 (2008) 2380–3239.
[24] K. Dincer, Experimental investigation of the effects of threefold type Ranque-Hilsch vortex tube and six cascade type Ranque-Hilsch vortex tube on the performance of counter flow Ranque-Hilsch vortex tubes, Int. J. Refrig. 34 (2011) 1366–1371.
[25] O. Aydın, M. Baki, An experimental study on the design parameters of a counterflow vortex tube, Energy 31 (2006) 2763–2772.
[26] B. Markal, O. Aydın, M. Avcı, An Experimental study on the effect of the valve angle of counter-flow Ranque-Hilsch vortex tubes on thermal energy separation, Exp. Therm. Fluid Sci. 34 (2010) 966–971.
[27] H. Pouraria, M.R. Zangooee, Numerical investigation of vortex tube refrigerator with a divergent hot tube, Energy Procedia 14 (2012) 1554–1559.
[28] R. Shamsoddini, A.F. Khorasani, A new approach to study and optimize cooling performance of a Ranque-Hilsch vortex tube, Int. J. Refrig. 35 (2012) 2339–2348.
[29] A. Berber, K. Dincer, Y. Yılmaz, D.N. Ozen, Rule-based Mamdani-type fuzzy modeling of heating and cooling performances of counter-flow Ranque-Hilsch vortex tubes with different geometric construction for steel, Energy 51 (2013) 297–304.
[30] M. Avcı, The effects of nozzle aspect ratio and nozzle number on the performance of the Ranque-Hilsch vortex tube, Appl. Therm. Eng. 50 (2013) 302–308.
[31] S.M. Acar, Thermodynamic Evaluation And Design Of Ranque-Hilsch Vortex Tube Aided Hybrid Cooling And Drying System, Dumlupinar University, Institute of Applied Sciences, 2016, (Ph.D. Thesis), Kutahya, Turkey (in Turkish).
[32] S.M. Acar, O. Arslan, The effect of cold stream of vortex tube on efficiency of the vapor compression refrigeration system, in: International Conference on Computational and Experimental Science and Engineering (ICCESEN-2014), October 25-29, Antalya, Turkey, 2014.
[33] F.C. Hooper, C.W. Ambrose, An improved expansion process for the vapour refrigeration cycle, in: Proc. 4th Canadian Congr. Applied Mechanics, Montreal, 1973, pp. 811–812.
[34] R.L. Collins, R.B. Lovelace, Experimental study of two-phase propane expanded through the Ranque-Hilsch tube, ASME J. Heat Transfer 101 (1979) 300–305.
[35] G.F. Nellis, S.A. Klein, The application of vortex tubes to refrigeration cycles, in: International Refrigeration and Air Conditioning Conference, Purdue University, USA, 2002, Paper 537.
[36] J. Sarkar, Exergy analysis of vortex tube expansion vapor compression refrigeration system, Int. J. Exergy 13 (4) (2013) 431–446.
[37] M. Okos, N. Rao, S. Drecher, M. Rode, J. Kozak, Energy usage in the food industry, American Council for an Energy-Efficient Economy, 1998, [Online] Available: http://www.aceee.org/pubs/ie981.htm, Accessed: 2014.
[38] S. Bell, A Beginner's Guide to Uncertainty of Measurement, Measurement Good Practice Guide 11, Issue 2, Centre for Basic, Thermal and Length Metrology National Physical Laboratory, UK, 1999.
[39] I. Doymaz, Air-drying characteristics of tomatoes, J. Food Eng. 78 (2007) 1291–1297.
[40] ASHRAE, Handbook of Refrigeration, Thermal properties of foods. ISBN 978-1-933742-82-3, American Society of Heating, Refrigerating and Air-Conditioning Engineers, Inc. 1791 Tullie Circle, N.E., Atlanta, GA, 2010, 30329.
[41] J. Ahrendts, Reference states, Energy 5 (1980) 667–677.
[42] A. Midilli, H. Kucuk, Energy and exergy analyses of solar drying process of pistachio, Energy 28 (2003) 539–556.
[43] T. Guler, M. Yucedag, Feasibility report of atmosphere controlled cold storage facility, Direct Business Support Program Fırat Development Agency, (in Turkish), 2011.
[44] A. Yogunlu, M. Yuzeroglu, S. Hopoglu, S.G. Gokce, The analysis and pre-feasibility of frozen fruit and vegetable sector, Fırat Development Agency, 2013, (in Turkish).
[45] http://isotsatisi.com/kategori-6-KURU_KISLIKLAR.html, The market price of dried tomatoes, (Last access: September 2015), (in Turkish).
[46] http://www.organikim.com.tr/organik-domates-kurusu-200-gr, The market price of dried tomatoes, (Last access: September 2015), (in Turkish).
[47] http://tazekuru.com/urunler/64/kurutulmus-domates-100g-?gclid=CLiLs–chMgCFSLnwgod-rgHiA, The market price of dried tomatoes (Last access: September 2015), (in Turkish).
[48] EMRA, June 29, 2015. Energy Market Regulatory Authority board decision. Decision No: 5666, Official Gazette of Turkish Republic No. 29401, (in Turkish).
[49] http://www.adana-bld.gov.tr/halfiyatlari.html, The price of fresh tomatoes, [Last access: September 2015] (in Turkish).
[50] http://www.tcmb.gov.tr/wps/wcm/connect/tcmb+tr/tcmb+tr/main+menu/duyurular/basin/2015/duy2015-13, CBRT (Central Bank of Republic of Turkish), Interest rate, (Last access: September 2015).
[51] http://www.tcmb.gov.tr/wps/wcm/connect/tcmb+tr/tcmb+tr/main+menu/para+politikasi/reeskont+ve+avans+faiz+oranlari, CBRT (Central Bank of Republic of Turkish), Discount rate, (Last access: September 2015).